Journal of Alloys and Compounds 550 (2013) 245–251

Contents lists available at SciVerse ScienceDirect

Journal of Alloys and Compounds

journal homepage: www.elsevier.com/locate/jalcom

Review

Influence of mineralizer agents on the growth of crystalline CeO_2 nanospheres by the microwave-hydrothermal method

R.C. Deus [a], M. Cilense [c,1], C.R. Foschini [c,1], M.A. Ramirez [a], E. Longo [c,1], A.Z. Simões [a,b,*]

[a] Universidade Estadual Paulista-Unesp – Faculdade de Engenharia de Guaratinguetá, Av. Dr. Ariberto Pereira da Cunha, 333 Bairro Portal das Colinas, CEP 12516-410 Guaratinguetá-SP, Brazil
[b] Universidade Federal de Itajubá-Unifei – Campus Itabira, Rua São Paulo, 377 Bairro Amazonas, CEP 35900-37 Itabira, MG, Brazil
[c] Universidade Estadual Paulista-Unesp – Instituto de Química – Laboratório Interdisciplinar em Cerâmica (LIEC), Rua Professor Francisco Degni s/n, CEP 14800-90 Araraquara, SP, Brazil

ARTICLE INFO

Article history:
Received 16 July 2012
Received in revised form 27 September 2012
Accepted 1 October 2012
Available online 11 October 2012

Keywords:
Nanoparticle
Chemical synthesis
Microwave
Electron microscopy
Crystal structure

ABSTRACT

Cystalline ceria (CeO_2) nanoparticles have been synthesized by a simple and fast microwave-assisted hydrothermal (MAH) under NaOH, KOH, and NH_4OH mineralizers added to a cerium ammonium nitrate aqueous solution. The products were characterized by X-ray powder diffraction (XRD), field-emission scanning electron microscopy (FE-SEM), transmission electron microscopy (TEM), Fourier Transformed-IR and Raman spectroscopies. Rietveld refinement reveals a cubic structure with a space group *Fm*3*m* while infrared data showed few traces of nitrates. Field emission scanning microcopy (FEG-SEM) revealed a homogeneous size distribution of nanometric CeO_2 nanoparticles. The MAH process in KOH and NaOH showed most effective to dehydrate the adsorbed water and decrease the hydrogen bonding effect leaving a weakly agglomerated powder of hydrated ceria. TEM micrographs of CeO_2 synthesized under MAH conditions reveal particles well-dispersed and homogeneously distributed. The MAH enabled cerium oxide to be synthesized at 100 °C for 8 min.

Contents

1. Introduction

Ceria (CeO_2) have been considered as important nanomaterial for applications in catalysts [1,2], fuel cells [3], ultraviolet absorbers [4], hydrogen storage materials [5], oxygen sensors [6], optical devices [7], polishing materials [8], and for which the use of nanocrystalline powders is an important factor. However, the high specific surface areas of nanocrystalline powders provide a stronger tendency of the powder to agglomerate. Weakly-agglomerated powder is needed both for dry processing methods, e.g. powder compaction, and for the preparation of stable suspensions in liquids, e.g. for thin or thick film production. Unless weakly-agglomerated nanoscale powders can be produced, the benefits expected from highly-uniform nanocrystalline powders are easily lost during the manufacture of components. The strength of

* Corresponding author at: Universidade Estadual Paulista-Unesp – Faculdade de Engenharia de Guaratinguetá, Av. Dr. Ariberto Pereira da Cunha, 333 Bairro Portal das Colinas, CEP 12516-410 Guaratinguetá-SP, Brazil. Tel.: +55 12 3123 2228/+55 31 3834 6472x6136; fax: +55 31 3834 6472/6136.
E-mail address: alezipo@yahoo.com (A.Z. Simões).
[1] Tel.: +55 16 3301 9828.

0925-8388/$ - see front matter © 2012 Elsevier B.V. All rights reserved.
http://dx.doi.org/10.1016/j.jallcom.2012.10.001

agglomerates depends on the surface properties of the nanocrystalline particles in the powder and these properties are sensitively dependent on the powder synthesis procedures [9]. Several methods have been developed to prepare ultrafine $Ce_{1-x}Gd_{xO2}$ powder, including hydrothermal [10], precipitation (for oxalate [11], carbonate [12,13], peroxide [9], hydroxide [14], polymeric precursor [15,16], complexion with citric acid [15], the flow method [17], organometallic decomposition [18] and microwave-assisted heating technique [19–21].

Among the various methods, the hydrothermal crystallization is an interesting process to directly prepare pure fine oxide powders with reduced contamination and low synthesis temperature. The microwave-assisted hydrothermal method requires longer soaking times at a low temperature (below 200 °C) to obtain the ceria powders. For this reason, the introduction of microwave heating to the conventional-hydrothermal method is advantageous for the synthesis of various ceramic powders because microwave heating permits a reduction of processing time and energy cost. Likewise, particles with desired size and shape can be produced if parameters such as solution pH, reaction temperature, reaction time, solute concentration and the type of solvent are carefully controlled [22]. A modification of the hydrothermal method developed by Komarneni et al. [23–25]. This method involves the introduction of microwave during the hydrothermal synthesis to increase the kinetics of crystallization by one to two orders of magnitude compared to the conventional hydrothermal. The microwave-assisted hydrothermal (MAH) method shows advantages such as rapidity, convenience and cost-effectiveness. Ceria systems with nanosized particles were successfully synthesized by the MAH method utilizing a relatively low temperature and short reaction time [26]. Here, the authors describe the formation conditions of ceria via the MAH method were reported in detail, and the advantages of microwave irradiation introduced.

As we have known, there are few works describing MAH route for the synthesis of pure CeO_2 nanoparticles. Gao et al. [27] report for the first time the preparation of ceria nanoparticles (1.6 nm) and nanorods (20 nm) under microwave-assisted conditions. Corradi et al. [28] also reported the synthesis of cubic CeO_2 crystals (5.7 nm) under microwave-assisted hydrothermal route around 194 °C for only 5 min. No calcination process or surfactant was required. The MAH method is getting very attractive in all areas of synthetic chemistry because it can boost some advantages over other synthetic methods [29]. This method has been extensively used in organic synthesis [30–32] and more recently this technique has also been widely applied to prepare inorganic nanostructured materials [33–36], with a wide range of applications [37–39]. In particular, Bilecka and Niederberger have been reported the versatility of the method for the synthesis of nanoparticles [40], while Baghbanzadeh et al. [41] have been presented a complete review on the subject. da Silva et al. [42] prepared $SrTi_{1-x}Fe_xO_3$ nanocubes by means of a MAH method at 140 °C. According to high-resolution transmission electron microscopy (HRTEM) results, these nanocubes are formed by a self-assembly process of small primary nanocrystals. In other paper of the group [43], $BaZrO_3$ (BZO) nanoparticles were nucleated, grown and subsequently self-assembled into a 3D decaoctahedronal architecture via a MAH method. A theoretical model based on the presence of uncoordinated bonds and/or charge distribution in the distorted constituent clusters (ZrO_6) and (BaO_{12}) of the material can be related to the change in both surface and internal defects during crystal growth. $BaZrO_3$ microcrystals were also obtained using the MAH at 140 °C for 40 min [44]. The growth mechanism for the formation of $BaZrO_3$ with decaoctahedron-shape was analyzed in detail, and the nature of the mechanism follows a non-classical growth process involving mesoscale self-assemblies of nanoparticles.

In this paper, we report the synthesis of CeO_2 nanospheres processed in a domestic microwave-hydrothermal oven. The focus is on the MAH efficiency to produce the CeO_2 nanoparticles as a function of the precipitant agents (KOH, NaOH and NH_4OH) solutions at lower temperatures and soaking times compared to the literature.

2. Experimental procedure

CeO_2 nanoparticles were synthesized by a hydrothermal microwave route. Cerium(IV) ammonium nitrate (5×10^{-3} mol L^{-1} $Ce(NH_4)_2(NO_3)_6$, 99.9% purity) was dissolved in 80 ml of deionized water under constant stirring for 15 min at room temperature. Subsequently, 1 ml of NH_4OH (30% in NH_3, Synth), 2 M NaOH (p.a, Merck) and 2 M KOH (p.a, Merck) was slowly added in the solution until the pH 10. The resulted solution was transferred into a sealed Teflon autoclave and placed in a hydrothermal microwave (2.45 GHz, maximum power of 800 W). The reactional system was heat treated at 100 °C/8 min with a heating rate fixed at 10 °C/min. The pressure in the sealed autoclave was stabilized at 1.2 atm. The autoclave was cooled to room temperature naturally. CeO_2 nanoparticles were collected and washed with acetone several times and then dried at 80 °C in a oven. The obtained nanoparticles were characterized by X-ray powder diffraction (XRD) using a (Rigaku-DMax/2500PC, Japan) with Cu-Kα radiation (λ = 1.5406 Å) in the 2θ range from 20° to 75° with 0.2 °/min. For Rietveld analyses, X-ray diffraction data were collected on a diffractometer under the following experimental conditions: 40 kV, 30 mA, $20° \leqslant 2\theta \leqslant 40°$, $\Delta 2\theta = 0.02°$, λCu kα monocromatized by a graphite crystal, divergence slit = 2 mm, reception slit = 0.6 mm, step time = 10 s. The crystallite size (d) of CeO_2 was calculated using Scherrer equation $d = k\lambda/\beta\cos\theta$, where k is constant, λ is wavelength of X-rays and β is the full width at half maximum (FWHM) for (1 1 1) reflection measured from slow scan where θ is the diffraction angle of the main peak. Raman spectra were collected (Bruker RFS-100/S Raman spectrometer with Fourier transform). A 1064 nm YAG laser was used as the excitation source, and its power was kept at 150 mW. The FT-IR spectra were recorded with a Bruker Equinox-55 instrument. Infrared spectroscopy was used for monitoring the structural changes occurring during the synthesis process with the KBr pellet technique. The morphology of as-prepared samples was observed using a high resolution field-emission gun scanning electron microscopy FEG-SEM (Supra 35-VP, Carl Zeiss, Germany). Specimens for TEM were obtained by drying droplets of as-prepared samples from an ethanolic dispersion which had been sonicated for 5 min onto 300 mesh Cu grids. TEM, HRTEM images and SAD patterns were then taken at an accelerating voltage of 200 kV on a Philips model CM 200 instrument. All measurements were taken at room temperature.

3. Results and discussion

3.1. X-ray diffraction analyses

The powder XRD patterns of as-prepared ceria nanoparticles showed the same crystalline structure for all the synthesis conditions used, Fig. 1. All of the peaks can be well-indexed to a pure cubic structure of CeO_2 (space group: $Fm3m$) with lattice constant a = 5.411 Å, which is in good agreement with the JCPDS file for

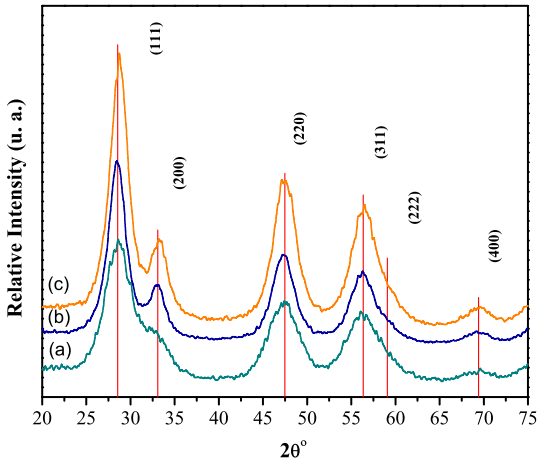

Fig. 1. X-ray diffraction pattern of CeO_2 nanoparticles synthesized at 100 °C for 8 min in the MAH method under different mineralizer agents: (a) KOH; (b) NaOH and (c) NH_4OH.

CeO_2 (JCPDS 34-394). It is worth noting that the overwhelmingly intensive diffraction peak is located at $2\theta = 28.660°$, which is from the [1 1 1] lattice plane of fcc CeO_2. No peak of any other phase is detected. The broadening of the peaks indicates that the crystallite sizes are small (4–9 nm), following the literature [45]. The average crystallite sizes calculated by Debye Scherrer is around 3.9; 5.8 and 9.1 nm for KOH; NaOH and NH_4OH, respectively. It is obvious that the mineralizer agents added on the solution, changes the CeO_2 crystal growth. As the average diffusion distance for the diffusing solute is short and the concentration gradient is steep in concentrated solutions, much diffusing material passes per unit time through a unit area [46]. Moreover, the average dimension of crystallites depends on the concentration of the precipitant agent solution: the higher the concentration of the mineralizer agent, the larger the ceria crystals. A clear evidence that CeO_2 is formed instead $Ce(OH)_x$ come from the fact that nitrate salts of ceria were preferably used since these salts were easily dissociable in few milliliters of water and the friable mass formed (Ce^{4+}) after treating with acid, reacted spontaneously with the mineralizer to produce a highly exothermic reaction. When cerium nitrate is used as the precursor salt and reacted with an acid to dissolve it, the Ce^{3+} ion is oxidized to Ce^{4+} ion and them acidic mass reacts exothermically with the mineralizer. It forms a by-product salt (KNO_3, $NaNO_3$ or NH_4NO_3) that surrounds the hydroxide product. In the oxidizing atmosphere, dehydration occurs, converting the hydroxide intermediate to oxide. In the MAH methods, the conversion to oxide is more rapid due to the effect of energetic radiations assisting the transformation to CeO_2 instead $Ce(OH)_x$.

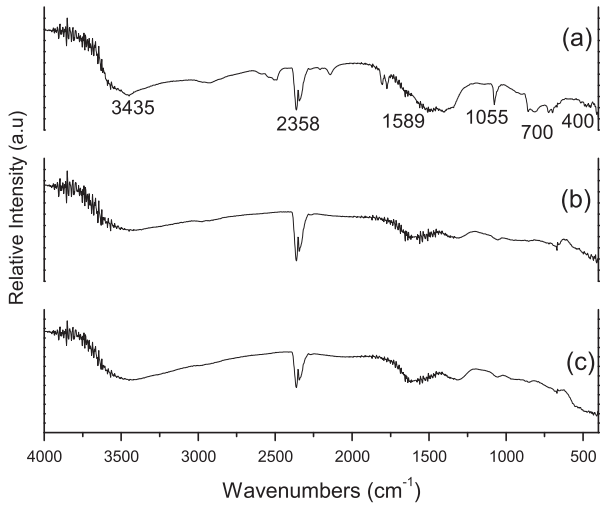

Fig. 3. FT-IR spectra of CeO_2 nanoparticles synthesized at 100 °C for 8 min in the MAH method under different mineralizer agents: (a) KOH; (b) NaOH and (c) NH_4OH.

Rietveld refinement technique was used to investigate the crystal structure of the CeO_2 nanoparticles obtained in the hydrothermal microwave at 100 °C for 8 min (see Fig. 2). All mineralizer agents indicated good quality of the refinement due its small difference between the experimental and theoretical lines. The atomic positions obtained by Rietveld analyses belong to the JCPDS

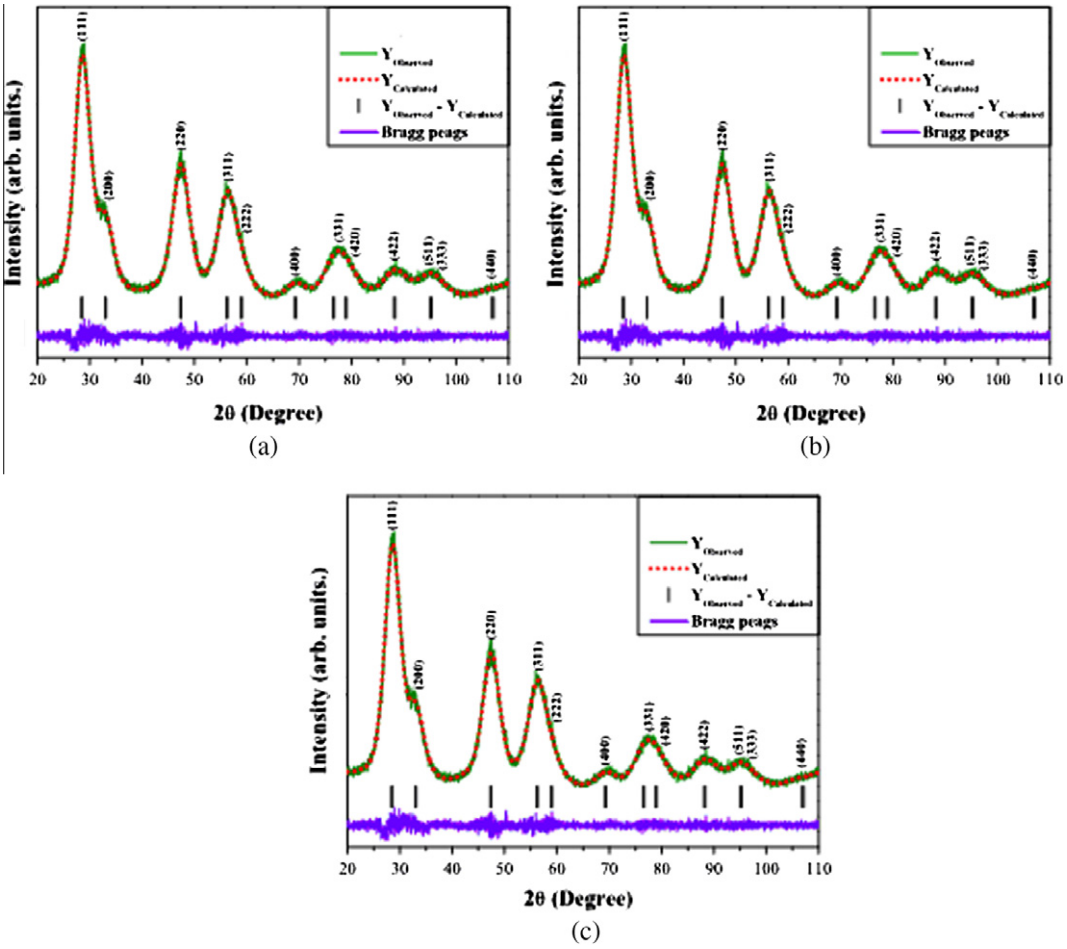

Fig. 2. Rietveld refinement of CeO_2 nanoparticles synthesized at 100 °C for 8 min in the MAH method under different mineralizer agents: (a) KOH; (b) NaOH and (c) NH_4OH.

file for CeO_2 (JCPDS 34-394) with a space group: *Fm*3*m*. The quantitative phase analyses for the cubic phase were calculated according to the reference of Young and Wiles [47]. The results obtained confirmed that the CeO_2 nanoparticles crystallized in the cubic phase with no changes during the refinement. From the low *S* values ($S = R_{wp}/R_{exp} = 1.2\%$) it can be assumed that the refinement of the CeO_2 particles obtained at 100 °C for 8 min in the MAH was successfully performed with all the investigated parameters close to literature data [48].

3.2. FT-IR and Raman analyses

Fig. 3 shows FTIR spectral features of CeO_2 samples. Strong intense bands at 3435, 2358, 1589 cm^{-1} and below 700 cm^{-1} were observed. The intense bands at 3435 and 1589 cm^{-1} correspond to the ν(O–H) mode of (H-bonded) water molecules and δ(OH), respectively. Residual water and hydroxy group are usually detected in the as-prepared ceria samples regardless of synthesis method used [49] and further heat treatment is necessary for their elimination. The FTIR spectrum of the ceria also exhibits strong broad band below 700 cm^{-1} which is due to the δ(Ce–O–C) mode. Specifically, the strong absorptive peaks at 400–600 cm^{-1} was attribute to the Ce–O stretching and bending vibration, being characteristics of the tetrahedral CeO_4 groups in the compounds. The hydroxylation and deprotonation of metal ions can be accelerated by raising the solution temperature or pressure [50]. A sharp band at 1385 cm^{-1} is indicative of N=O stretching vibration. This peak indicates traces of nitrate. The peak at 1055 cm^{-1} and are attributed to the vibrations associated with the incoordination of the adsorbed NO_3^{-1} ions [51]. Band in the 2358 cm^{-1} region was attributed to the stretching frequency of the acetone group. That suggests that the acetone group was chemically bonded to the surface of the ceria nanocrystals. This is probably the result of reactions forming chemical bonds between the nanocrystal surface and the organic-ligand molecule in the unique reaction conditions of supercritical water, which are essential for the perfect dispersion of nanocrystals in organic solvents and for the arrangement of individual nanocrystals into superlattices and new studies should be performed to avoid it's presence. The crystallized nanoparticle was found to have OH^- ions due to the alkali used in the present reaction conditions. Furthermore, the hydroxyl content was found to change with the mineralizaer agent which could be due to the vigorous action of microwaves to remove these groups at elevated temperatures during the hydrothermal process. In hydrothermal-microwave processing, the high frequency electromagnetic radiation interacts with the permanent dipole of the liquid (H_2O) which initiates rapid heating from the resultant molecular rotation. Also, permanent or induced dipoles in the dispersed phase cause rapid heating of the particles which results in a reaction temperature in excess of the surrounding liquid-localized superheating. Following the literature, hydrolysis refers to those reactions of metallic ions with water that liberate protons and produce hydroxide or oxide solids. Ce^{4+} ions, which have a low basicity and high charge, undergo strong hydration. Firstly, Ce^{4+} ions are hydrolyzed and form complexes with water molecules or OH^- to give $[Ce(OH)_x(H_2O)_y]^{(4-x)+}$, where $x + y$ is the coordination number of Ce^{4+}. Further polymerization is likely, and both species can serve as the precursors for the final ceria nanoparticles. In an aqueous solution, H_2O, being a polar molecule, tends to take protons away from coordinated hydroxide, leading to the formation of $CeO_2\ nH_2O$. This process can be described by the following equations [52]:

$$Ce^{4+} + xOH + yH_2O \rightarrow [Ce(OH)_x(H_2O)_y]^{(4-x)+} \quad (1)$$

$$[Ce(OH)_x(H_2O)_y]^{(4-x)+} + H_2O \rightarrow CeO_2 \cdot nH_2O + nH_2O + H_3O^+ \quad (2)$$

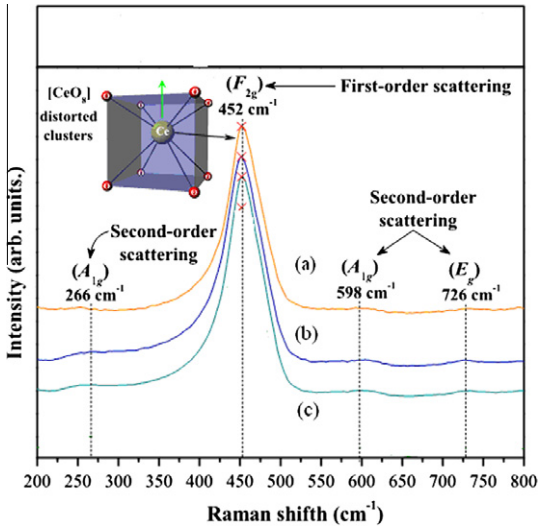

Fig. 4. Raman spectra of CeO_2 nanoparticles synthesized at 100 °C for 8 min in the MAH method under different mineralizer agents: (a) KOH; (b) NaOH and (c) NH_4OH.

Raman scattering has proven to be a valuable technique to obtain information about local structures within materials. To confirm the formation of pure ceria, FT-Raman spectrum was obtained (see Fig. 4). Cubic fluorite structure-metal dioxides have a single Raman mode at 464.5 cm^{-1}, which has F2 g symmetry and can be viewed as a symmetric breathing mode of the O atoms around each cation. Since only the O atoms move, the vibrational mode is nearly independent of the cation mass [53,54]. The fast structural organization of CeO_2 particles processed in MAH can be related to the heating process which occurs from the interior to the surface. The microwave energy is transformed into heat through the interaction between molecules and atoms with the electromagnetic field. This interaction results in an internal and volumetric heating of the powders which promotes the formation of temperature gradients and heat flows.

As shown, three additional low intensity second scattering Raman bands are detected around 266, 598 and 726 cm^{-1}, respectively. These bands are usually assigned to the presence of extrinsic oxygen vacancies generated into the ceria lattice improving diffusion rate of bulk oxygen.

3.3. FE-SEM and TEM analyses

FEG-SEM micrographs of CeO_2 obtained at different mineralizer agents are shown in Fig. 5. According to the image, most of the grains of CeO_2 powders are homogeneous with an average particle size calculated from the FE-SEM images of 11.5; 8.8 and 6.7 nm for KOH; NaOH and NH_4OH, respectively. However, CeO_2 powders obtained in NH_4OH agents reveal smaller particles which display poor contrast and intense agglomeration amongst extremely fine particles. Aggregation between the particles decreases and monodispersed particles are observed in the case of KOH and NaOH mineralizers agent. The higher agglomeration degree increased in NH_4OH mineralizer agent due to the $-OH$ ligand derived from NH_4OH to make the metal hydroxide precursor. In this case, all of the $-OH$ and $-OOH$ ligands formed $Ce(OH)_x(OOH)_{4-x}$ precursor which was transformed to CeO_2 after hydrothermal treatment and Van der Waal's force may be responsible for the formation of CeO_2 agglomerates. Moreover, the distribution in size seemed to be homogeneous and the shape appeared rounded. The synthesized ceria particles were relatively spherical with uniform size distribution, which was observed by FEG-SEM. Nanometric and

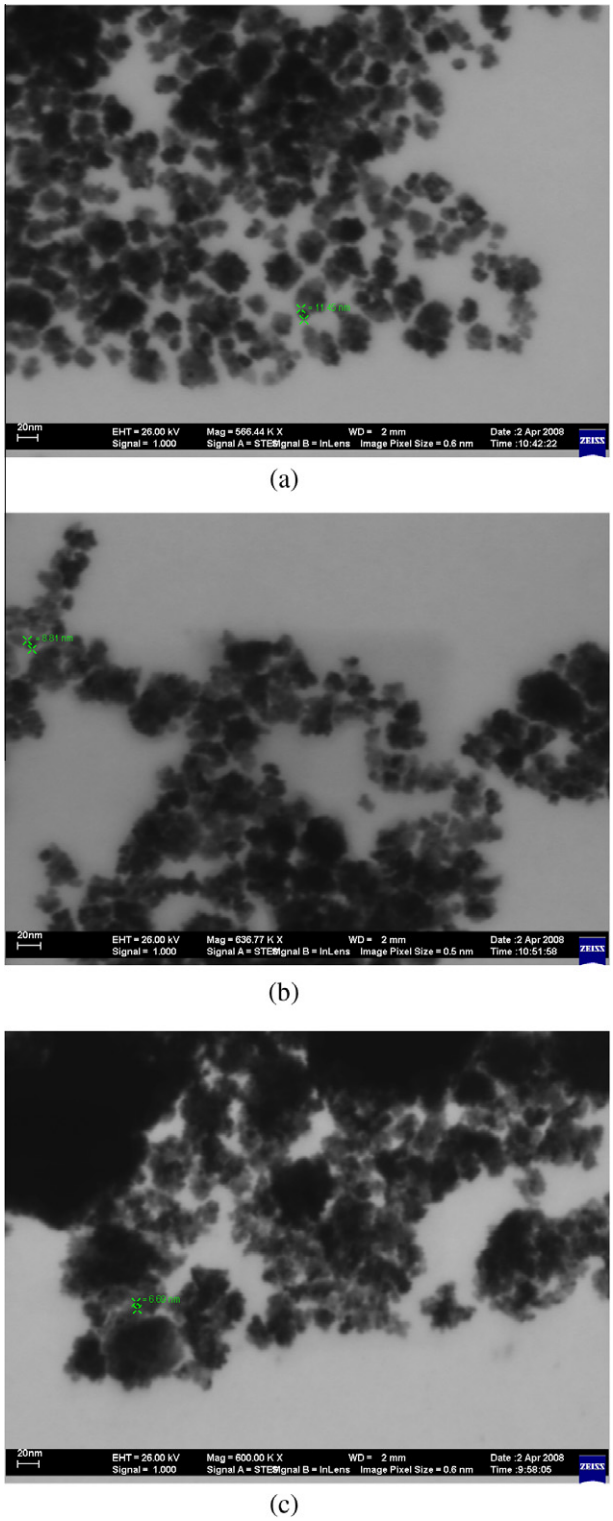

Fig. 5. FEG-SEM spectra of CeO_2 nanoparticles synthesized at 100 °C for 8 min in the MAH method under different mineralizer agents: (a) KOH; (b) NaOH and (c) NH_4OH.

isotropic CeO_2 crystallites obtained in this study are quite different from the previous study, where CeO_2 powders agglomerated into a cubic shape with the side size of 4.8 nm under hydrothermal conditions [55]. In the hydrothermal process, the presence of an alkaline medium was found to be essential. In our case, a critical mineralizer agent could exist above which the formation of agglomerates was favored, and the formation of weak agglomerated CeO_2 was highly dependent upon this formation. The "dissolution and crystallization" process can be utilized to describe the hydrothermal reaction [56]. During the hydrothermal treatment, Ce^{4+} or Ce^{3+} hydroxides underwent an attack by basic medium to dissolve and react at high temperatures and pressures, and then precipitated as insoluble ceramic oxide particles from the supersaturated hydrothermal fluid. If the temperature and pressure conditions are carefully maintained during the duration of the experiment, neither etching of CeO_2 crystals nor the formation of agglomerates is observed. Therefore, the dissolution and crystallization process continued in supersaturated fluid in such a way that the system was self-stabilizing. We conjecture that the dissociation of cerium hydroxide and the formation of ionic complexes might prevent the growth of CeO_2 crystallites and limit the size of particles to the nanometric range. The agglomeration process was attributed to Van der Waals forces. To reduce the surface energy, the primary particles have a tendency to form nearly spherical agglomerates, in a minimum surface to volume ratio [57]. This type of grain structure is common in oxide, ferrite and titanate ceramics [58,59] which is a result of an abnormal/discontinuous grain particle and also called an exaggerated grain particle. In abnormal growth, some particles grow faster than others with increasing sintering temperature. Abnormal grain particles may results from: (1) the existence of second phase precipitates or impurities, (2) materials with high anisotropy in interfacial energy and (3) materials with high chemical equilibrium [60]. In hydrothermally derived CeO_2 which crystallizes in a cubic structure it can be assumed that the abnormal grain particles comes from factor (2) and (3) due the existence of high chemical equilibrium. The random aggregation process between the small particles can be related to an increase in effective collision rates between small particles by microwave radiation [61] which indicates that microwave energy favors an anisotropic growth caused by the differences in the surface energies on the different crystallographic faces [62]. Possibly, the imperfections or differences between the particles size can be associated with the influence of microwave energy during the CeO_2 phase growth process.

The particle size of the CeO_2 powders was also examined using the TEM (Fig. 6). CeO_2 synthesized by MAH under NaOH and NH_4OH at 100 °C for 8 min, revealing the particle sizes are approximately range from 6 to 8 nm (Fig. 6b and c). The resultant particles have a spherical shape with approximately 6 nm in diameter. However, Fig. 6a presents TEM micrographs of CeO_2 synthesized under MAH conditions on KOH mineralizer agent. The particle size was higher (11 nm) with diameters of 4 nm and are homogeneously distributed compared to previous condition. The small size of the CeO_2 particles synthesized by MAH under NH_4OH can be explained quite simply. It is postulated that at the start of the reaction a large number of nucleus forms in the solution and as the reaction takes place in a very dilute solution there is not enough reactant left for the growth of the particles. As a result, the particles do not grow beyond 7 nm. After annealing on NH_4OH agent, the large agglomerates disappeared and became smaller isometric ones and the maximum particle size decreased sharply attaining a value of 7 nm. There was not obvious change in the morphology under MAH conditions. The MAH treatment on NH_4OH proved to be uneffective condition to decrease the agglomerate. In this condition, the as-prepared CeO_2 nanoparticle showed a larger amount of water. Usually, particles surfaces adsorb water molecules, so that hydrogen bonds can be formed between approaching particles. Therefore, hydrogen bonding can lead to hard agglomerates of particles during the drying and calcining process. The MAH process at KOH and NaOH showed most effective to dehydrate the adsorbed water and decrease the hydrogen bonding effect leaving a weakly agglomerated nanoparticles of hydrated ceria. Alternatively, if the solution was

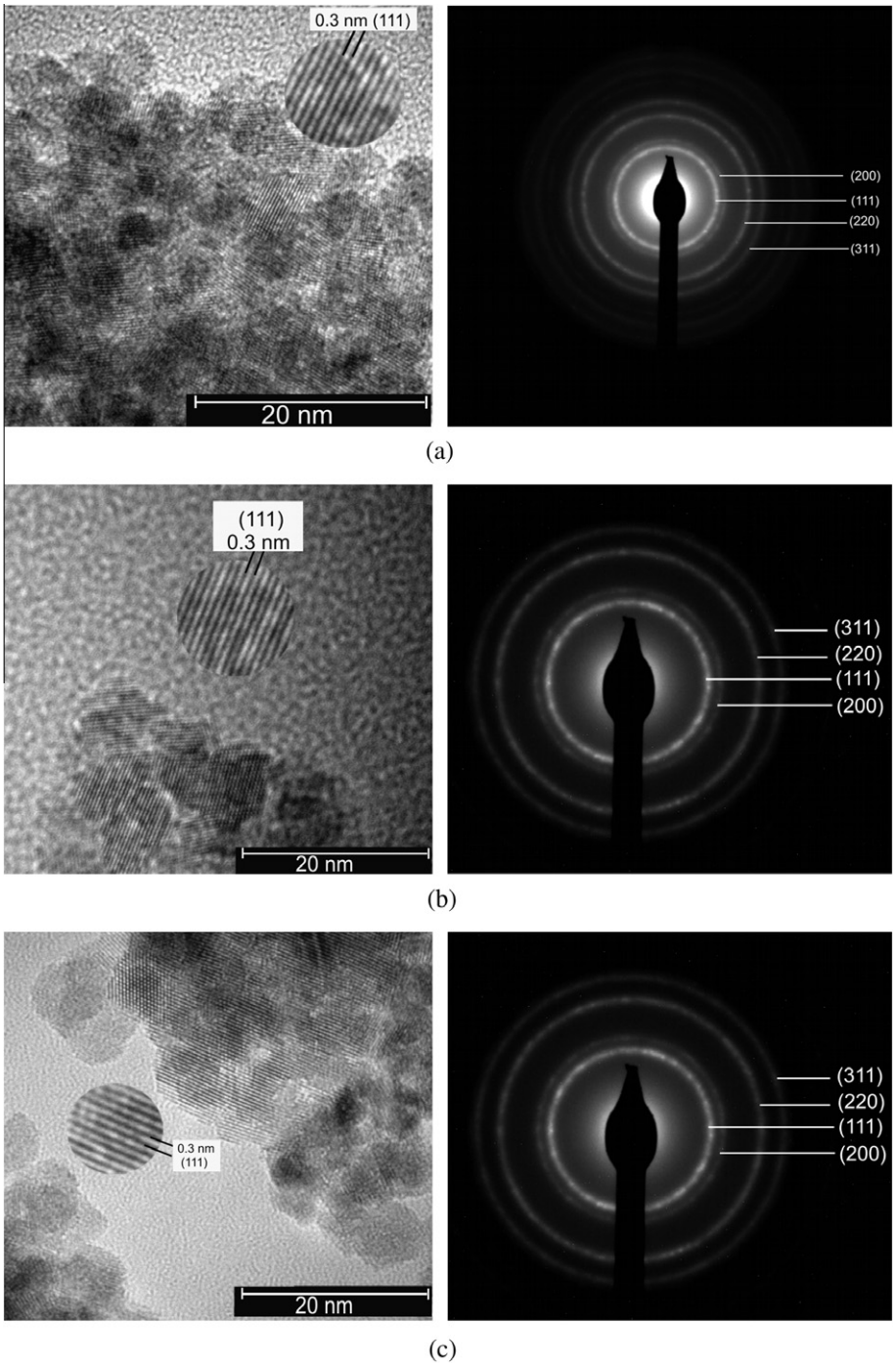

Fig. 6. TEM images of CeO_2 nanoparticles synthesized at 100 °C for 8 min in the MAH method under different mineralizer agents: (a) KOH; (b) NaOH and (c) NH_4OH.

maintained at basicity, it might be due to crystallization from amorphous gel through a dissolution-precipitation, because solubility of cerium hydroxide is very high in the strong basic solution.

4. Conclusions

Adopting the microwave-hydrothermal process as synthesis method it is possible to obtain, by treating the solution at 100 °C for only 8 min, nanometric and crystalline ceria nanoparticles. The hydrothermal reaction to grow CeO_2 crystallites with a pure phase being described by the dissolution–crystallization process. Rietveld refinement reveals a cubic structure with a space group *Fm*3*m*. FEG-SEM analyses have shown a homogeneous size distribution of nanometric CeO_2 crystallites. Raman scattering revealed first scattering mode typical of cubic fluorite structure while second scattering Raman modes are assigned to the presence of extrinsic oxygen vacancies generated into the ceria lattice. CeO_2 synthesized by MAH under NH_4OH revealed agglomerate particles while CeO_2 synthesized under MAH conditions on KOH and NaOH mineralizers agent were well-dispersed and homogeneously distributed. This can be explained by the amount of hydrogen bonds during the drying and calcining process to hard agglomerates of particles. The MAH process at KOH and NaOH showed most effective to dehydrate the adsorbed water and decrease the hydrogen bonding effect leaving a weakly agglomerated nanoparticle of hydrated ceria. MAH is important not only for the use of a short

treatment time and low temperature but also for the possibility to control the morphological and structural properties. Therefore, the MAH method is undeniably a genuine technique for low temperatures and short times in comparison with the previous methodologies.

Acknowledgements

The financial support of this research project by the Brazilian research funding agencies CNPq and FAPESP is gratefully acknowledged. We also gratefully acknowledged Professor José Arana Varela and Diogo Volanti for TEM facilities, Elane Paris for Rietveld analyses and Laécvio Cavalcante for Raman measurements.

References

[1] B.M. Reddy, A. Khan, Y. Yamada, T. Kobayashi, S. Loridant, J.C. Volta, Langmuir 19 (7) (2003) 3025–3030.
[2] P. Bera, A. Gayen, M.S. Hegde, N.P. Lalla, L. Spadaro, F. Frusteri, F. Arena, Journal of Physical Chemistry B 107 (25) (2003) 6122–6130.
[3] G. Jacobs, L. Williams, U. Graham, D. Sparks, B.H. Davis, Journal of Physical Chemistry B 107 (38) (2003) 10398–10404.
[4] R.X. Li, S. Yabe, M. Yamashita, S. Momose, S. Yoshida, S. Yin, T. Sato, Solid State Ionics 151 (1–4) (2002) 235–241.
[5] K. Sohlberg, S.T. Pantelides, S.J. Pennycook, Journal of the American Chemical Society 123 (27) (2001) 6609–6611.
[6] P. Jasinski, T. Suzuki, H.U. Anderson, Sensors and Actuators B-Chemical 95 (1–3) (2003) 73–77.
[7] F. Goubin, X. Rocquefelte, M.H. Whangbo, Y. Montardi, R. Brec, S. Jobic, Chemistry of Materials 16 (4) (2004) 662–669.
[8] D.G. Shchukin, R.A. Caruso, Chemistry of Materials 16 (11) (2004) 2287–2292.
[9] B. Djuricic, S. Pickering, Journal of the European Ceramic Society 19 (11) (1999) 1925–1934.
[10] S. Dikmen, P. Shuk, M. Greenblatt, H. Gocmez, Solid State Sciences 4 (5) (2002) 585–590.
[11] S.W. Zha, C.R. Xia, G.Y. Meng, Journal of Power Sources 115 (1) (2003) 44–48.
[12] Y.R. Wang, T. Mori, J.G. Li, T. Ikegami, Journal of the American Ceramic Society 85 (12) (2002) 3105–3107.
[13] J.G. Li, T. Ikegami, Y.R. Wang, T. Mori, Journal of the American Ceramic Society 86 (6) (2003) 915–921.
[14] M.J. Godinho, R.F. Goncalves, L.P.S. Santos, J.A. Varela, E. Longo, E.R. Leite, Materials Letters 61 (8–9) (2007) 1904–1907.
[15] R.A. Rocha, E.N.S. Muccillo, Advanced Powder Technology III 416 (4) (2003) 711–717.
[16] S. Wang, K. Maeda, Journal of the American Ceramic Society 85 (7) (2002) 1750–1752.
[17] F. Bondioli, A.B. Corradi, T. Manfredini, G. Leonelli, R. Bertoncello, Chemistry of Materials 12 (2) (2000) 324–330.
[18] H.Z. Song, H.B. Wang, S.W. Zha, D.K. Peng, G.Y. Meng, Solid State Ionics 156 (3) (2003) 249–254.
[19] H. Wang, J.J. Zhu, J.M. Zhu, X.H. Liao, S. Xu, T. Ding, H.Y. Chen, Physical Chemistry Chemical Physics 4 (15) (2002) 3794–3799.
[20] H.M. Yang, C.H. Huang, A.D. Tang, X.C. Zhang, W.G. Yang, Materials Research Bulletin 40 (10) (2005) 1690–1695.
[21] M.M. Natile, G. Boccaletti, A. Glisenti, Chemistry of Materials 17 (25) (2005) 6272–6286.
[22] J.S. Lee, S.C. Choi, Materials Letters 58 (3–4) (2004) 390–393.
[23] S. Komarneni, R. Roy, Q.H. Li, Materials Research Bulletin 27 (12) (1992) 1393–1405.
[24] S. Komarneni, Q. Li, K.M. Stefansson, R. Roy, Journal of Materials Research 8 (12) (1993) 3176–3183.
[25] S. Komarneni, Q.H. Li, R. Roy, Journal of Materials Chemistry 4 (12) (1994) 1903–1906.
[26] S. Komarneni, R. Pidugu, Q.H. Li, R. Roy, Journal of Materials Research 10 (7) (1995) 1687–1692.
[27] F. Gao, Q. Lu, S. Komarneni, Journal of Nanoscience and Nanotechnology 6 (12) (2006) 3812–3819.
[28] A.B. Corradi, F.B. Bondioli, A.M. Ferrari, T. Manfredini, Materials Research Bulletin 41 (1) (2006) 38–44.
[29] T.N. Glasnov, C.O. Kappe, Chemistry A European Journal 17 (43) (2011) 11956–11968.
[30] A. De la Hoz, A. Díaz-Ortiz, A. Moreno, Chemical Society Reviews 34 (2005) 164–178.
[31] C.O. Kappe, Angewandte Chemie International Edition 43 (2004) 6250–6284.
[32] T.L.C. Martins, T.C.C. França, C. Teodorico, T.C. Ramalho, ; J.D.F. Villar, Synthetic Communications (34) (2004) 3891–3899.
[33] I. Bilecka, M. Kubli, E. Amstad, M. Niederberger, Journal of Sol-Gel Science and Technology 57 (2011) 313–322.
[34] M. Estruga, C. Domingo, J.A. Ayllon, Research Bulletin 45 (2010) 1224–1229.
[35] V. Abdelsayed, A. Aljarash, M.S. El-Shall, Chemistry of Materials 21 (2009) 2825–2834.
[36] M. Baghbanzadeh, S.D. Skapin, Z.C. Orel, C.O. Kappe, Chemistry A European Journal 18 (2012) 5724–5731.
[37] S.-E. Park, Journal of Physics and Chemistry of Solids. (69) (2008) 1501–1504.
[38] S. Saremi-Yarahmadi, B. Vaidhyanatha, International Journal of Hydrogen Energy 35 (2010) 10155–10165.
[39] R.G. Deshmukh, S.S. Badadhe, I.S. Mulla, Research Bulletin 44 (2009) 1179–1182.
[40] I. Bilecka, M. Niederberger, Nanoscale 2 (2010) 1358–1374.
[41] M. Baghbanzadeh, L. Carbone, P.D. Cozzoli, Angewandte Chemie International Edition 50 (2011) 11312–11359.
[42] L.F. Silva, W. Waldir Avansi, M.L. Moreira, A. Juan, E. Longo, V.R. Mastelaro, CrystEngComm (14) (2012) 4068–4073.
[43] M.L. Moreira, A. Juan, V.R. Mastelaro, V.R. Varela, J.A. Longo, CrystEngComm (13) (2011) 5818–5824.
[44] L.R. Macario, M.L. Moreira, A. Juan, L. Longo, CrystEngComm 12 (2010) 3612–3619.
[45] B. Djuricic, S. Pickering, Journal of the European Ceramic Society 19 (1999) 1925–1934.
[46] H.R. Tan, J.P.Y. Tan, C. Boothroyd, T.W. Hansen, Y.L. Foo, M.J. Lin, Journal of Physical Chemistry C 116 (2012) 242–247.
[47] R.A. Young, A. Sakthivel, T.S. Moss, C.O. Santos, Paiva, Journal of Applied Crystallography (28) (1995) 66–367.
[48] K. Zhou, Z. Yang, S. Yang, Chemistry of Materials 19 (2007) 1215–1217.
[49] H. Wang, J.J. Zhu, J.M. Zhu, X.H. Liao, S. Xu, T. Ding, Physical Chemistry (4) (2002) 794–3799.
[50] G.J. Wilson, A.S. Matijasevich, D.R.G. Mitchell, J.C. Schulz, G.D. Will, Langmuir 22 (2006) 2016–2027.
[51] Y.W. Zhang, S. Rui, C.S. Liao, C.H. Yan, Journal of Physical Chemistry B 107 (2003) 10159–10163.
[52] M. Hirano, M. Inagaki, Journal of Materials Chemistry 10 (2) (2000) 473–477.
[53] J.R. McBride, K.C. Hass, B.D. Poindexter, W.H. Weber, Journal of Applied Physics 76 (1994) 2435–2441.
[54] P. Fornasiero, G. Balducci, R. DiMonte, J. Kaspar, V. Sergo, G. Gubitosa, Journal of Catalysis 164 (1996) 173–183.
[55] R. Lee Pen, J.F. Banfield, Science 281 (1998) 969–971.
[56] Y.B. Khollam, A.S. Deshpande, A.J. Patil, H.S. Potdar, S. Deshpande, B.S. Date, Materials Chemistry and Physics 71 (2001) 304–308.
[57] J. Yoo, The Effects of Microstructure on $Ba_{1-x}Sr_xTiO_3$ Pyroelectric Materials for Pyroelectric and Bolometer Infrared Sensors, Ph.D. Thesis, University of Auckland, 1999.
[58] A.Z. Simões, E.C. Aguiar, A.H.M. Gonzalez, J. Andrés, E. Longo, J.A. Varela, Journal of Applied Physics (104) (2008) 104115-1–104115-6.
[59] A.Z. Simões, L.S. Cavalcante, C.S. Riccardi, J.A. Varela, E. Longo, Current Applied Physics (9) (2009) 520–523.
[60] S.-J.L. Kang, Sintering Densification, Grain Growth & Microstructure, Elsevier, Oxford, 2005. p. 265.
[61] M. Godinho, C. Ribeiro, E. Longo, E.R. Leite, Crystal Growth & Design (8) (2008) 384–386.
[62] J. Geng, Y. Lv, D. Lu, J.-J. Zhu, Nanotechnology 17 (2006) 2614–2620.